Bulletin of the Geological Survey of Japan, vol.55 (3/4), p. 93- 103 , 2004

DMAP.m: A Mathematica® program for three-dimensional mapping of tortuosity and porosity of porous media

Yoshito Nakashima[1] and Tetsu Yamaguchi[2]

Yoshito Nakashima and Tetsu Yamaguchi (2004) DMAP.m: A Mathematica® program for three-dimensional mapping of tortuosity and porosity of porous media. *Bull. Geol. Surv. Japan*, vol. 55 (3/4), 93-103, 10 figs, 3 tables.

Abstract: We developed a Mathematica® program for three-dimensional mapping of the porosity and normalized apparent diffusion coefficient (tortuosity) of isotropic heterogeneous porous media. The program, DMAP.m, is a package-type program for Mathematica® version 4 or later. DMAP.m accepts three-dimensional (3D) digital image data for the porous media as an input. Such data may be obtained by, for example, X-ray computed tomography (CT) as a set of text files of two-dimensional contiguous CT slices (square matrices). DMAP.m reads the text files and divides the image set into sub-cubes, then executes a non-sorbing random walk (lattice walk) through the discrete pore space in each sub-cube. A specified number of voxels are chosen randomly as the start position of the random walk. If the chosen voxel falls within a pore, random walk simulation is carried out until the walker exits the sub-cube. If the chosen voxel falls within a solid, the random walk is not performed. The porosity of each sub-cube is calculated as the probability of a successful hit on a pore voxel in this random choice of the start position (Monte Carlo integral). The time required for the walkers to escape from each sub-cube is recorded in the random walk simulation, representing an "out-diffusion" or "out-leaching" numerical simulation. The tortuosity (apparent diffusion coefficient in the free space divided by that in porous media) is calculated by fitting the time-dependent cumulative number of walkers that have escaped from the sub-cube to a theoretical curve. DMAP.m was applied successfully here to the 3D X-ray CT image of a monosized sand pack. DMAP.m is available for free download on the author's website (URL = http://staff.aist.go.jp/nakashima.yoshito/progeng.htm) to facilitate study on porous media by X-ray CT or nuclear magnetic resonance imaging.

Keywords: Apparent Diffusion Coefficient, Formation Factor, Nuclear Magnetic Resonance Imaging (MRI), Pore Structure, Random Walk, Tortuosity, X-ray CT

1. Introduction

Diffusion or random walk through pores is the predominant migration mechanism for groundwater and contaminants in geological systems with small Péclet numbers. Geological systems (*e.g.*, water-saturated porous soils or rocks) are usually heterogeneous, and the transport properties of such porous media vary significantly from position to position within the system (*e.g.*, Gibbs *et al.*, 1993). Thus, it is important to map the three-dimensional (3D) distribution of transport properties (*e.g.*, diffusivity and porosity) in order to fully understand the processes involved in contaminant hydrogeology. It is now possible to obtain high-resolution 3D digital images of heterogeneous porous structures through the use of techniques such as X-ray computed tomography (CT) and nuclear magnetic resonance imaging (MRI) (*e.g.*, Gleeson and Woessner, 1991; Wildenschild *et al.*, 2002; Nakashima and Watanabe, 2002). A computer program can then be needed to obtain the 3D distribution of diffusivity and porosity using such digital images. To the best of the author's knowledge, however, no such programs have been made publicly available at little or no cost. Thus, in the present study, we developed an original Mathematica® program for 3D mapping of the tortuosity (normalized apparent diffusivity) and porosity of heterogeneous porous media.

This program, DMAP.m, is a package-type program for Mathematica® version 4 or later. DMAP.m reads a 3D image set, and divides the set into subsystems which are then mapped in terms of diffusivity and porosity. Random walkers migrate through the discrete pore space in each subsystem by avoiding the solid obstacles. The time required for the walkers to escape from the subsystem is recorded to calculate the apparent diffusion coefficient of the porous subsystem. A specified number of voxels are chosen randomly as the

[1] Institute for Geo-Resources and Environment, GSJ, AIST, Higashi 1-1-1 Central7, Tsukuba, Ibaraki 305-8567, Japan.
[2] Marketing Group, Visualization Business, KGT Inc., 2-8-8 Shinjuku Shinjuku-ku, Tokyo 160-0022, Japan.

start positions of the random walk. The porosity of each subsystem is then calculated as the probability that the chosen voxels are pore voxels (Monte Carlo integral). DMAP.m has been briefly introduced by Nakashima and Yamaguchi (2004), and applied to a CT image set of a porous sandstone by Nakashima *et al.* (2004). However, the detail of the algorithm and theoretical background has not been described. In this paper, we describe the detail of the DMAP.m program and the results of a trial application using 3D X-ray CT images of a monosized sand pack to demonstrate the program performance. This program is available for free download from the author's website (URL = http://staff.aist.go.jp/nakashima.yoshito/progeng.htm) to facilitate study on porous media using X-ray CT and MRI.

2. Transport properties of porous media

The terminology of the transport properties of isotropic porous media is explained here using the Kozeny-Carman model (*e.g.*, Guéguen and Palciauskas, 1994). The Kozeny-Carman model is a fluid-saturated equiradii pipe network through which fluid/tracer molecules migrate by diffusion or Poiseuille flow (Fig. 1). The porosity, ϕ, refers to the volume fraction of the pipes in the porous cube:

$$\phi = \frac{n\pi r^2 l}{l_0^3} \tag{1}$$

where l is the pipe length, r is the radius of the cylindrical pipe, and n is the number of cylindrical pipes in the l_0^3 cube (Nakashima and Yamaguchi, 2004).

The diffusion coefficient is defined as the ratio of the diffusion flux to the concentration gradient (Fick's first law; *e.g.*, Crank, 1975). The tortuosity of the water-saturated porous media is the degree of the elongation of the pipe, and is defined as $(l/l_0)^2$ in Fig. 1. Because the diffusion obeys a parabolic partial differential equation, $(l/l_0)^2$ is equal to D_{bulk}/D where D_{bulk} is the diffusion coefficient of the tracer in the bulk fluid (*i.e.*, ϕ=1) and D is the apparent diffusion coefficient of the tracer in the fluid-saturated porous media (*e.g.*, Latour *et al.*, 1993; Nakashima and Watanabe, 2002):

$$\left(\frac{l}{l_0}\right)^2 = \frac{D_{bulk}}{D} \tag{2}$$

In general, D_{bulk}/D will be larger than unity because the solid component of the porous media is an obstacle to the tracers diffusing through the pore space.

The formation factor (normalized electrical resistivity) of porous rocks and sediments saturated with conductive fluid is an important quantity in geophysical exploration (*e.g.*, Jinguuji and Kunimatsu, 1999; Jinguuji *et al.*, 2003). Assuming a Kozeny-Carman model for the pore structure (Fig. 1), it is possible to calculate the formation factor using the porosity and tortuosity as follows. For bulk fluid system (*i.e.*, $\phi = 1$), the resistance of the l_0^3 cube is ρ/l_0 where ρ is the resistivity of the bulk fluid. For the Kozeny-Carman model with $\phi \neq 1$, it is $\rho l/(n\pi r^2/3) = 3\rho l^2/(\phi l_0^3)$, calculated using Eq. (1) and the assumption that one-third of the pipes are parallel (*i.e.* run in the same direction). The factor 3 is derived from this assumption. The formation factor, F, is defined as the ratio of the resistances mentioned above:

$$F = \frac{3\rho l^2/(\phi l_0^3)}{\rho/l_0} = \frac{3}{\phi}\left(\frac{l}{l_0}\right)^2 = \frac{3}{\phi}\left(\frac{D_{bulk}}{D}\right) \tag{3}$$

where $(l/l_0)^2 = D_{bulk}/D$ is the tortuosity (Eq. (2)). Because $F = 1$ and $D_{bulk}/D = 1$ for bulk fluid system (*i.e.*, porous media of $\phi = 1$), it is required that $F \to 1$ as $\phi \to 1$ and $D_{bulk}/D \to 1$. Thus, the numerical constant, 3, in the right-hand side of Eq. (3) should be omitted to obtain

$$F \approx \frac{1}{\phi}\left(\frac{D_{bulk}}{D}\right) \tag{4}$$

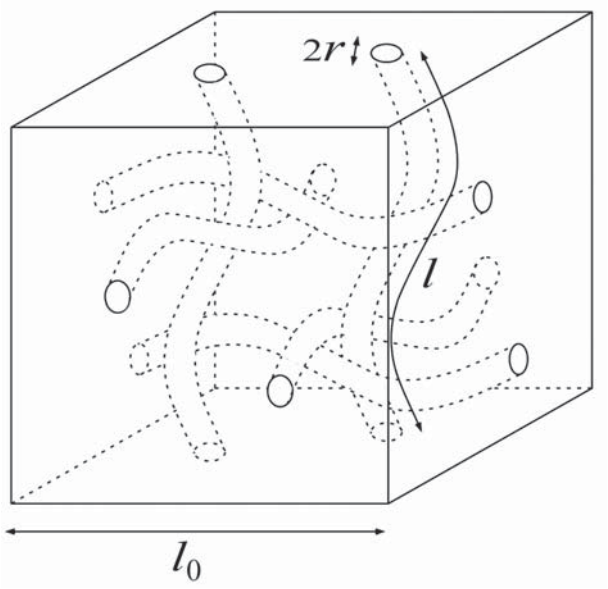

Fig. 1 Kozeny-Carman model of the pore structure in a cubic porous medium for the estimate of the formation factor. Equiradii cylindrical pipes (diameter $2r$) run orthogonally. The pipes are completely filled with conductive fluid (resistivity ρ), and the resistivity of the solid is infinite. The pipe length is l in the cube of l_0^3, and thus the tortuosity of the pipes is $(l/l_0)^2$.

This is the final expression of the formation factor using the porosity and tortuosity.

3. Out-diffusion of non-sorbing tracers in porous media

The theory of non-sorbing tracer diffusion in isotropic water-saturated porous media is reviewed here briefly. DMAP.m simulates conventional "out-diffusion" or "out-leaching" laboratory experiments using non-sorbing random walkers. The relevant mathematical expression for the out-diffusion experiment is as follows. A tracer-rich water-saturated porous cubic sample of side length a is immersed in a large container filled with tracer-free bulk water at $t = 0$, where t is time. The resultant escape of the tracer particles from the cube into the container is monitored as a function of t. The tracer concentration, c, obeys the following parabolic partial differential equation:

$$\frac{\partial c}{\partial t} = D\left(\frac{\partial^2 c}{\partial x^2} + \frac{\partial^2 c}{\partial y^2} + \frac{\partial^2 c}{\partial z^2} \right) \quad \text{for } 0 \le x,y,z \le a \tag{5}$$

where x, y, and z are the spatial coordinates, and D is the apparent diffusion coefficient of the non-sorbing tracer. The initial condition is set as

$$c(x,y,z,t) = c_0 \qquad \text{at} \quad t = 0 \tag{6}$$

where c_0 is a constant. It is assumed that tracer particles disappear as soon as they escape from the porous cube. Thus, the boundary condition is given by

$$c(x,y,z,t) = 0$$
on the six faces of the cube (*i.e.*, x,y, or $z = 0$ or a) (7)

It is straightforward to solve Eqs. (5)-(7) analytically by separation of variables. As a result, the exact solution for the cumulated flux of tracer, $M(t)$, emergent from the six faces of the cube is expressed by:

$$M(t) = c_0 a^3 - \int_0^a \int_0^a \int_0^a c(x,y,z,t)\,dx\,dy\,dz$$

$$= \frac{512 M(\infty)}{\pi^6} \sum_{n_1=1,3,5,7,\ldots}^{\infty} \sum_{n_2=1,3,5,7,\ldots}^{\infty} \sum_{n_3=1,3,5,7,\ldots}^{\infty} \frac{1}{n_1^2 n_2^2 n_3^2} \left(1 - \exp\left[-\frac{D\pi^2}{a^2} (n_1^2 + n_2^2 + n_3^2) t \right] \right)$$

$$= M(\infty) - \frac{512 M(\infty)}{\pi^6} \left[\sum_{n_1=1,3,5,7,\ldots}^{\infty} \frac{\exp\left(-\frac{D\pi^2 n_1^2 t}{a^2} \right)}{n_1^2} \right]^3 \tag{8}$$

where $M(\infty)$ is $c_0 a^3$. In the early stages, Eq. (8) reduces to Eq. (9), indicating that $M(t)$ increases linearly with the square-root of time (Hespe, 1971):

$$M(t) \propto \left(\frac{S}{V} \right) \sqrt{Dt} \qquad \text{as } t \to 0 \tag{9}$$

where (S/V) is the surface-to-volume ratio of the sample (*e.g.*, $(S/V) = 6/a$ for the cube).

Fitting the experimental data to Eq. (9) is performed in conventional out-diffusion experiments (Hespe, 1971; Siitari-Kauppi *et al.*, 1997; Sardini *et al.*, 2003). However, using only the $M(t)$ data for the early stages implies that pore structure information from deep inside the cube is discarded, precluding calculation of the diffusion coefficient averaged over the cubic system. Another drawback is that the number of data points obeying Eq. (9) is small, which may lead to significant statistical estimation errors. Thus, the original form, Eq. (8), was fitted to the simulation results in this study to estimate the apparent diffusion coefficient.

4. The DMAP.m program

The original program DMAP.m simulates the out-diffusion of non-sorbing tracers in sub-cubes of porous media. DMAP.m is a package-type program for Mathematica® version 4 or later. The program list of DMAP.m, an example of program execution (Mathematica® Notebook), and usage notes 'readme.txt' are available at the author's website (URL =http://staff.aist.go.jp/nakashima.yoshito/progeng.htm). An example of program execution is also given in Table 1. Refer to the usage notes (readme.txt) for details of how to use DMAP.m.

DMAP.m (i) reads data on a three-dimensional porous structure as a set of text files of two-dimensional images in a directory, (ii) performs a lattice walk in the pore space, and (iii) exports the simulation results (*e.g.*, integrated flux, M) as text files. The input parameters and output files are listed in Tables 2 and 3, respectively.

In process (i), DMAP.m accepts 3D digital image data on the porous media obtained by, for example, X-ray CT as a set of text files of contiguous two-dimensional CT slices (square matrices). The digital image should be cubic in terms of both spatial resolution (*i.e.*, voxel dimension) and total system size. It should be noted that binary files (*e.g.*, TIFF images) cannot be processed by DMAP.m and should be converted to text files without headers using, for example, Graphic Converter (http://www.lemkesoft.de/en/graphcon.htm). DMAP.m reads the text files to divide the image set into sub-cubes (Fig. 2). For example, if the image consists of 256^3 voxels and the variable

Table 1 Example of the execution of DMAP.m program. The electronic file (Mathematica® Notebook) of Table 1 is available for free download at the author's website.

```
In[1]:=  << DMAP`

In[2]:=  Timing[
          DMAP["C:\\temp\\dmap\\256text", 2,
           NumberOfDivision→3,
           PixelRange→ {-1, 58.5},
           NumberOfWalkers→30000,
           MaxTime→ 20000,
           TimeDataFileDirectory→ "C:\\temp\\dmap\\allTout",
           CumulateDataFileDirectory→"C:\\temp\\dmap\\cumulate",
           OutputFileDirectory→ "C:\\temp\\dmap",
           Verbose→ True]
         ]
```

Table 2 Explanation of parameters used in Table 1.

Parameter	Meaning
Timing	Return the CPU time used
C:\\temp\\dmap\\256text	Directory where 3D image data (set of 2D text files) are located
2	Integer parameter k for the calculation of T_{out}
NumberOfDivision	Number of division of the cube
PixelRange	Minimum and maximum values of the gray-level of pore space
NumberOfWalkers	Number of trails of choosing voxels as the start positions of the lattice walk
MaxTime	Maximum number of the lattice-walk time step
C:\\temp\\dmap\\allTout	Directory where simulation results (T_{out}) are saved
C:\\temp\\dmap\\cumulate	Directory where simulation results (cumulated flux) are saved
C:\\temp\\dmap	Directory where simulation results (except for T_{out} and cumulated flux) are saved
Verbose -> True	Show the current status of the program execution step by step

Table 3 Explanation of output text files.

File name	Contents
cumulated	Cumulated flux, $M(\tau)$, for $1 \leq \tau \leq$ MaxTime
tout	T_{out} of all lattice walk trials
TimeOverWalkers	Number of the lattice walk trials in which walkers still remain in the sub-cube at τ = MaxTime
TimeAverage	Averaged T_{out}
DiffusionCoeffs	(sub-cube size)^2/TimeAverage where "sub-cube size" = a/(voxel dimension)
PoreRatio	Porosity (in vol.%) calculated by Eq. (10)
PoreWalkers	Hit number of the pore voxels in the random choice of the start position

NumberOfDivision in Table 2 is 2, $2^3 = 8$ sub-cubes are generated (each sub-cube consists of 128^3 voxels). If NumberOfDivision = 3, $3^3 = 27$ sub-cubes are generated ($256 = 3\text{x}85 + 1$), each consisting of 85^3 voxels, and the residual $256^3 - 27\text{x}85^3 = 195{,}841$ voxels are discarded. The random walk simulations are performed in each sub-cube to obtain the spatial distribution of the diffusion coefficients and porosities.

The details of the algorithm of process (ii), which forms the main part of the program, are as follows. The random walk algorithm is a lattice walk in a simple cubic lattice, and walkers migrate via discrete voxels with gray-levels corresponding to pore space. A voxel in a sub-cube is chosen randomly as a start position for the lattice walk at $\tau = 0$ where τ is dimensionless integer time. The walker executes a random jump to

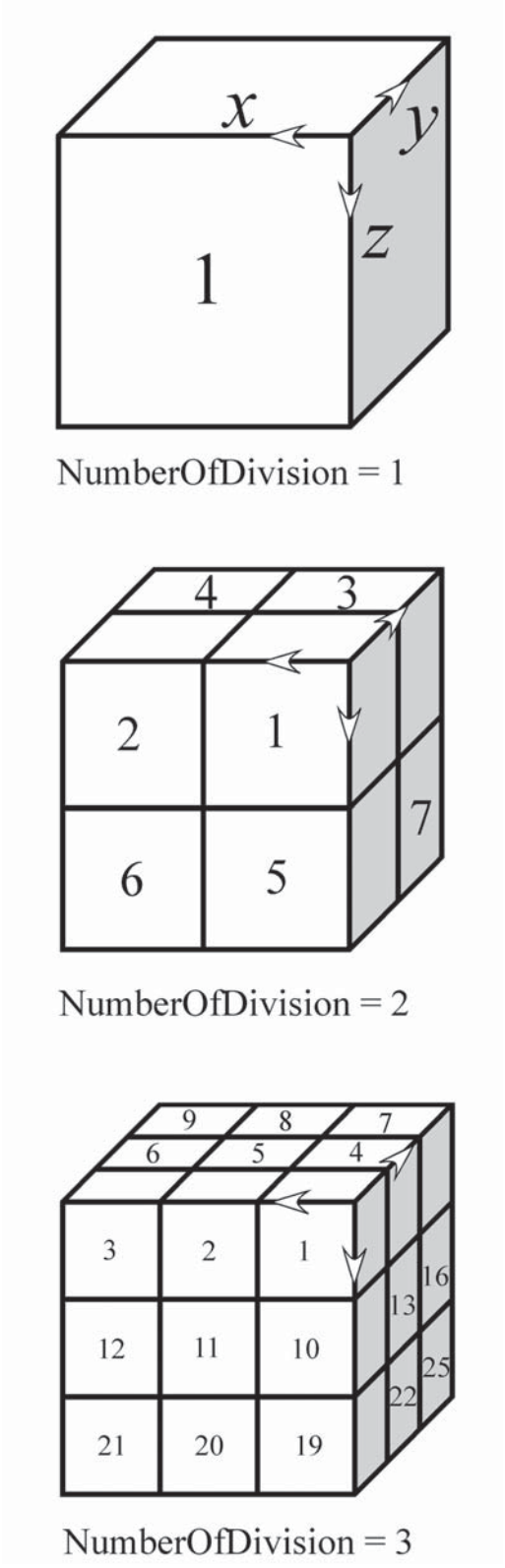

Fig. 2 Rule concerning the division of sub-cubes. Division starts from the origin (x, y, z) = (0, 0, 0) of the right-handed coordinate system, and ends at the corner farthest from the origin. Examples of the generated sub-cubes with serial sub-cube numbers are shown for NumberOfDivision = 1, 2, and 3.

one of the six nearest unoccupied sites, and τ is incremented by unit time after the jump to advance the time to τ +1. If the randomly selected site or voxel is occupied by an obstacle or solid, the jump is not performed, but the time is incremented to τ +1 (*e.g.*, Stauffer, 1985). Because DMAP.m calculates the geometrical tortuosity of the pore structure, the random walkers are assumed to be non-sorbing, and no electrochemical interaction (*e.g.*, sorption) between the walkers and solid obstacles is considered.

If the pore space in which a walker is located is connected to the surface of the sub-cube, the walker eventually escapes from the sub-cube. The quantity T_{out} (dimensionless integer time required for walkers to escape from the sub-cube) is recorded to calculate the cumulated flux, $M(\tau)$, of the walkers that escaped from the sub-cube in time, τ. The apparent diffusion coefficient, D, for the sub-cube is estimated by fitting $M(\tau)$ to a theoretical curve, as given by Eq. (8). It is also possible to calculate D_{bulk} for the sub-cube if PixelRange (intensity range of voxels through which walkers can migrate) in Table 2 is sufficiently large to cover the intensity range of both pore space and solid. Thus, D_{bulk}/D can be calculated for each sub-cube. In this way, DMAP.m can be used for a three-dimensional mapping of tortuosity.

Although the main function of DMAP.m is to calculate the tortuosity, the porosity of the sub-cube is also obtained as a byproduct. A large number of voxels are chosen randomly as a start position for the lattice walk. If the chosen voxel falls within a pore, the random walk simulation is carried out until the walker exits the digital CT image system. If the chosen voxel falls within a solid, the random walk will not be performed. The porosity of each sub-cube is then calculated as the probability that the start position is a pore in this random choice process (Monte Carlo integral).

The apparent diffusion coefficient could also be calculated by taking the time-derivative of the mean-square displacement of random walkers (*e.g.*, Nakashima and Watanabe, 2002). For a successful simulation, this algorithm requires that a (system size of the sub-cube) is sufficiently large to satisfy the relation: (pore size/voxel dimension)^2 << random walk time step << (a/voxel dimension)^2 (Watanabe and Nakashima, 2002). However, this condition often breaks down in the DMAP.m program because the image system is divided into small sub-cubes of similar dimensions to the pore size. Hence, $M(\tau)$ was calculated in DMAP.m, and D was estimated by fitting $M(\tau)$ to Eq. (8).

The input parameters required to execute DMAP.m as shown in Table 1 are explained in Table 2. The parameter, NumberOfWalkers, should be as large as possible to ensure reliable simulation, otherwise the stochastic nature of the random walk and Monte Carlo

integral reduce the accuracy of the calculated tortuosity and porosity. Each lattice walk trial stops (i) if the voxel chosen as the start position is a solid voxel, (ii) when the walker escapes from the sub-cube, or (iii) when τ reaches MaxTime. MaxTime should be set appropriately for a successful simulation: if MaxTime is too low, walkers cannot escape from the sub-cube. A low multiple of (a/voxel dimension)^2 should be reasonable as the MaxTime value, representing the characteristic time required for walkers to escape from a sub-cube of $\phi = 1$ (*i.e.*, no obstacles). If a voxel in an isolated pore is chosen as the start position of the lattice walk, the walker is confined in the pore region and never leaves the sub-cube, resulting in an infinite T_{out} where T_{out} is an integer time required for a walker to escape from the sub-cube. In order to avoid this numerical difficulty, when the time step, τ, exceeds MaxTime, the lattice walk is terminated and T_{out} is taken to be MaxTime +1. Thus, a lattice walk trial of T_{out} = MaxTime +1 suggests that the walker is confined in an isolated pore, and should be discarded in the calculation of tortuosity because only a random walk through the percolation cluster of pore space in the cubic system can contribute to long-distance macroscopic material transport across the system.

The program outputs are listed in Table 3. Raw T_{out} data are saved in a text file named "tout". The most important output is the time-dependent cumulated flux, $M(\tau)$. By fitting $M(\tau)$ to Eq. (8) it is possible to estimate D of the sub-cube. A nonzero TimeOverWalkers would suggest that some walkers were trapped in isolated pores. The undesirable effect of isolated pores mentioned above is negligible in the estimate of D using Eq. (8) because $M(\tau)$ is for $1 \leq \tau \leq$ MaxTime, whereas T_{out} of walkers in isolated pores is MaxTime +1 (*i.e.*, out of range of the $M(\tau)$ data).

The *total porosity* of each sub-cube is calculated using the entries in the output files of Table 3 according to the Monte Carlo integral:

$$\phi = \frac{\text{PoreRatio}}{100} = \frac{\text{PoreWalkers}}{\text{NumberOfWalkers}} \qquad (10)$$

It should be noted that both isolated pores and pores connected to the surface of the sub-cube contribute to this porosity value. On the other hand, the quantity defined by

$$\phi = \frac{M(\text{MaxTime})}{\text{NumberOfWalkers}} \qquad (11)$$

gives the *effective porosity* of only pores connected to the surface of the sub-cube. Users are requested to choose Eq. (10) or (11) depending on the purpose of the study.

One limitation is related to adsorption on the solid surface. There are two possible reasons for a tortuosity greater than unity: (i) high geometrical complexity of the porous structure and (ii) bound or less mobile walkers absorbed on the solid surface. The effects of absorption on the solid surface are neglected in the program at present, and as such renders the program inapplicable to systems such as H_2O self-diffusion in porous clay gels (Nakashima, 2003ab), where the effects induced by bound water near negatively charged clay surfaces are not negligible. Another limitation is related to the anisotropy of the porous media. The porous structure is assumed to be isotropic in the tortuosity calculation, and thus D is a scalar. Therefore, the program is not applicable to highly anisotropic porous samples (*e.g.*, schist), where D is a tensor, rather than a scalar.

5. Application to a sand pack

In order to demonstrate the capabilities of DMAP.m, the program was used to estimate the tortuosity and porosity of a monosized sand pack. The monosized sand pack was chosen as a good analogue of well-sorted natural sandy sediments. The sand sample used was granodioritic sand grains collected at the coast of Uchinoura, Kagoshima, Japan. The dominant mineral species of the sand were quartz, feldspar, biotite, and cummingtonite. The sand sample was sieved, so that the grain size is 0.85–1.18 mm in diameter. The sand grains were packed in a plastic cylinder, and the 3D images were obtained by microfocus X-ray CT (Nakashima and Yamaguchi, 2004).

An X-ray CT image of a randomly packed pile of the sand grains is shown by Fig. 3. The 8-bit voxel intensities of the sand grains and air-filled pores are high and low, corresponding to high and low density, respectively. According to Nakashima and Yamaguchi (2004), the ranges of voxel intensity of the pores and grains were set at 0-58 and 59-255, respectively. The cluster labeling analysis using this threshold value for the discrimination of grains and pores revealed that the total porosity was 0.34 and effective porosity (*i.e.*, porosity of the largest pore cluster) was 0.33 (Nakashima and Yamaguchi, 2004). A free program, Kai3D.m (Watanabe *et al.*, 1999; Nakashima and Watanabe, 2002), was used for the cluster labeling analysis. The analysis also revealed 323 isolated small pores in the 3D image system probably derived from the noise in the CT system or from the small pores in sand grains. The 323 isolated pores (total 1573 voxels) are responsible for the slight difference between the total porosity (0.34) and effective porosity (0.33), but should be disused in terms of the calculation of the tortuosity of the 256^3 image system because the macroscopic material transport across the 256^3 system is performed on the largest pore cluster.

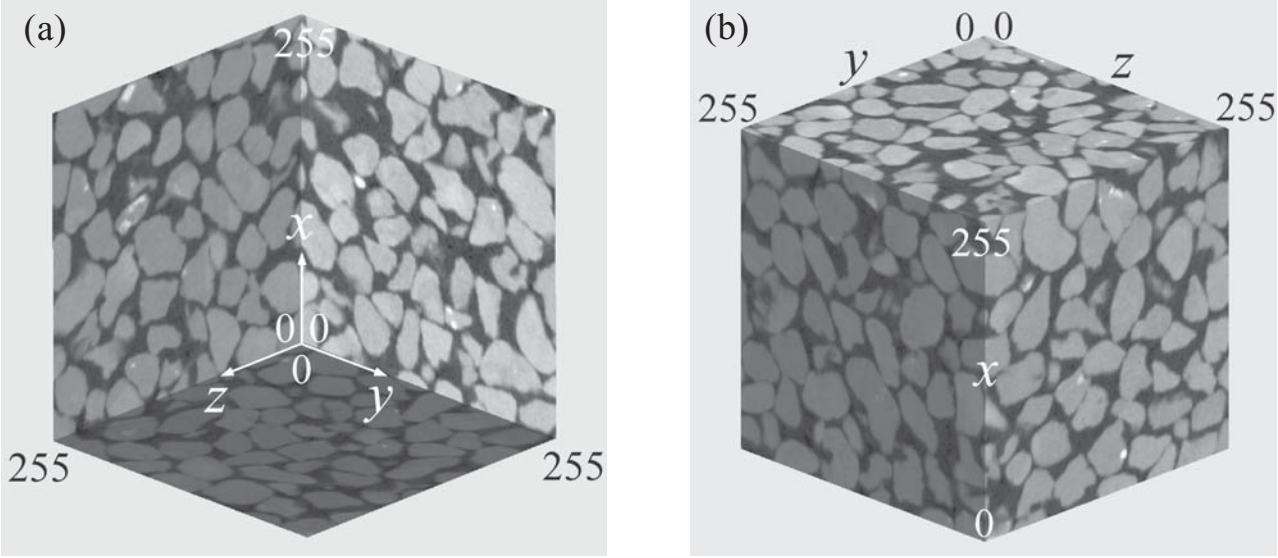

Fig. 3 Three-dimensional X-ray CT image of a monosized (diameter 0.85-1.18 mm) sand pack. 256x256x256 voxels ≈ 7.3x7.3x7.3 mm^3. (a) Front view. (b) Rear view. The 8-bit voxel-intensity ranges from black (0) to white (255).

In this section, the obtained $M(\tau)$ data were fitted to the following theoretical curve according to Eq. (8):

$$M(\tau) = \frac{512M(\mathrm{MaxTime})}{\pi^6}\left(\frac{\pi^6}{512} - \exp[-K\tau] - \frac{1}{3}\exp\left[-\frac{11K\tau}{3}\right] - \frac{2212}{18225}\exp[-9K\tau] - \frac{1}{27}\exp\left[-\frac{19K\tau}{3}\right]\right) \quad \text{as } \tau \to \infty \tag{12}$$

where $K \propto 3\pi^2 D/a^2$. The cumulated flux at τ = MaxTime, M(MaxTime), is in the entry of the output file, "cumulated". Eq. (12) was obtained by choosing the first 5 terms from the infinite series in Eq. (8). Because the truncated terms disappear rapidly as $\tau \to \infty$ owing to the large decay constant, Eq. (12) is a reasonable approximation for large τ . The tortuosity D_{bulk}/D was then calculated using dimensionless K as follows.

$$\frac{D_{bulk}}{D} = \frac{K_{bulk}}{K} \tag{13}$$

where K_{bulk} is K for the lattice walk in free space (*i.e.*, $\phi = 1$).

To evaluate the general features of the out-diffusion phenomena, DMAP.m was first applied to out-diffusion from a free space ($\phi = 1$) without dividing the image system (Fig. 4). The CPU time was 19 hours for this simulation using a personal computer (Mathematica® ver. 4.1 on Microsoft Windows XP® with Pentium® 4 processor of 1.5 GHz). The flux decreased with time (Fig. 4a) and the cumulated flux approached a constant value (Fig. 4b). This is a characteristic feature of the diffusion process. It is difficult in Fig. 4b to distinguish the simulation data and the fitted curve (Eq. (12)) owing to the high accuracy of the fit. Therefore, Fig. 4b demonstrates that Eq. (12) is useful for analyzing the simulation data. Eq. (9) was then fitted to exactly the same data (Fig. 4c), revealing that Eq. (9) is applicable only for short times ($\tau^{1/2} < 50$). The characteristic migration distance of walkers (root-mean-square displacement) is $\tau^{1/2}$ for the lattice walk in a simple cubic lattice if the lattice constant is unity. Therefore, if D is determined using only the data set for $\tau^{1/2} < 50$, the D value obtained is the diffusivity of the pore structure very close to the surface of the cube (50 voxels in depth from each surface). Thus, data analysis using Eq. (9) fails to probe the pore structure deep inside the 256^3 cube, demonstrating the advantage of Eq. (12) over Eq. (9).

The results of the lattice walk through the pore space in the 256^3 cube are shown in Fig. 5. The CPU time was 11 hours for this simulation using the same personal computer mentioned above. In this case, PoreWalkers = 10009 and NumberOfWalkers = 30000, and the total porosity defined by Eq. (10) is PoreWalkers/NumberOfWalkers = 10009/30000 ≈ 0.33. The ratio of the "in the sand pack" $M(\tau)$ to the "in the free space" $M(\tau)$ as $\tau \to \infty$ in Fig. 5 is equal to the effective porosity. TimeOverWalkers was only 4 and M(MaxTime) is 10005, indicating that the effective porosity calculated by Eq. (11) is 10005/30000 ≈ 0.33. According to the cluster labeling analysis, the total porosity was 0.34 and effective porosity was 0.33. These values agree well with the results obtained by

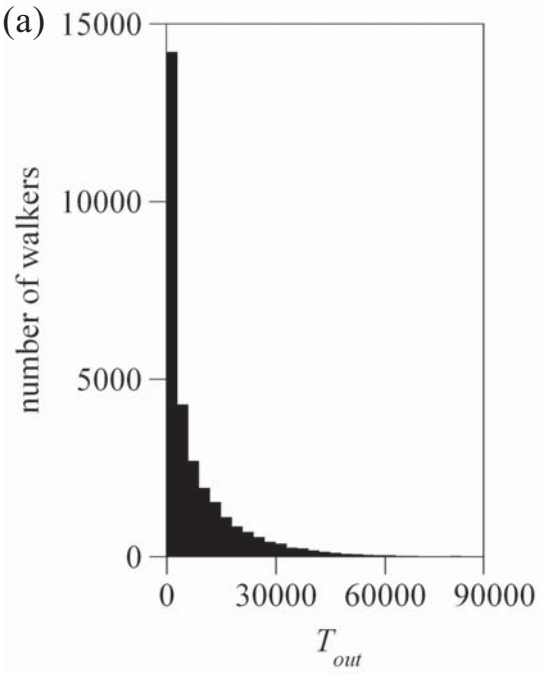

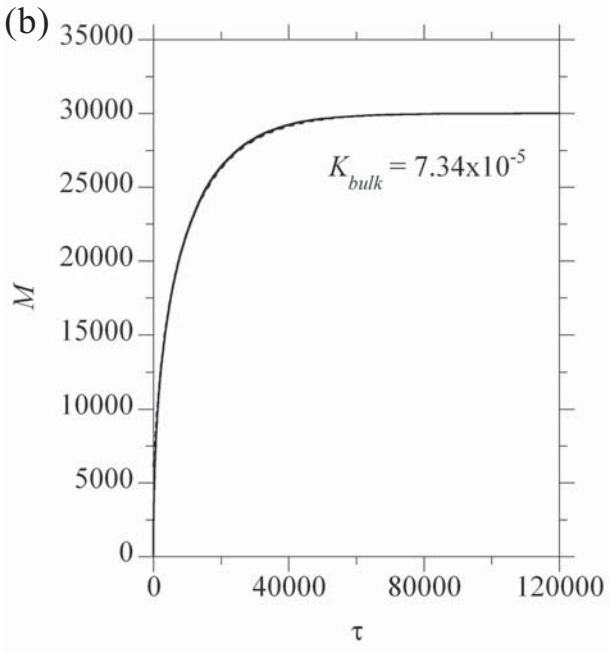

Fig. 4 Results for the lattice walk simulation in free space (ϕ = 1). NumberOfDivision =1, NumberOfWalkers = 30000 and MaxTime = 300000. (a) Histogram of T_{out}. Each column is 3000 wide. TimeAverage = 8072. (b) Cumulated flux, M, as a function of τ. The simulation result (solid line) was fitted using a model (Eq. (12), broken line) to obtain K_{bulk} = 7.34x10^{-5}. (c) Cumulated flux, M, as a function of $\tau^{1/2}$. The simulation result (solid line) was fitted using a model (Eq. (9), broken line). Note that fitting the data to Eq. (9) is good only for the earliest time stage ($\tau^{1/2}$ < 50).

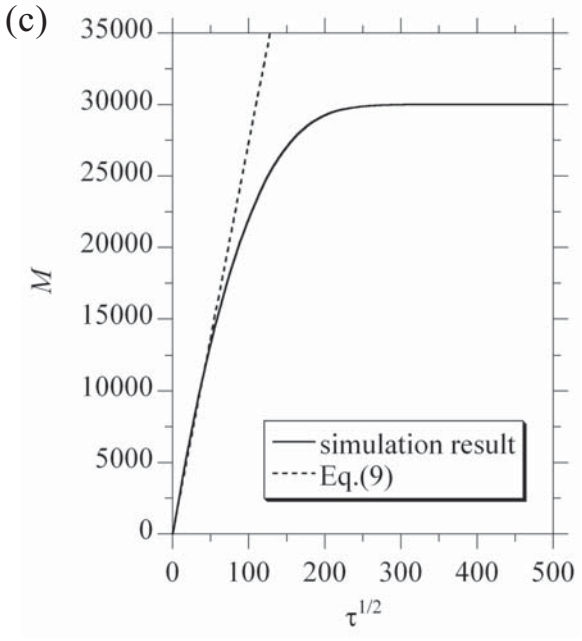

DMAP.m. From Fig. 5, the tortuosity calculated by Eq. (13) was K_{bulk}/K = 7.34x10^{-5}/3.99x10^{-5} = 1.84. On the other hand, the tortuosity calculated using the time-derivatives of the mean-square displacement of walkers is 1.84 for the same image data of 256^3 voxels (Nakashima and Yamaguchi, 2004). The tortuosity value again agrees well with the result obtained by DMAP.m, demonstrating that DMAP.m is capable of probing the pore structure of porous media accurately.

Three-dimensional mapping of the porosity and tortuosity was performed using Eqs. (10) and (13), respectively (Fig. 6). The value of NumberOfDivision was set at 1-3, corresponding to 1^3, 2^3, and 3^3 sub-cubes (Fig. 2). Data for the early stage of the walk satisfying $M(\tau)/M$(MaxTime) < 0.25 were discarded, and the remaining data was fitted to Eq. (12) in order to reduce the error derived from the truncation. The CPU time used was, for example, 24 hours for NumberOfDivision = 3. Fig. 6 shows that the degree of scatter in the data increased as the sub-cube size decreased. This is due to the local heterogeneity of the pore structure within the 256^3 cube. Fig. 6 also shows that the tortuosity increased with decreasing porosity. This relationship between tortuosity and porosity has been confirmed through laboratory experiments and numerical simulations (*e.g.*, Nakashima, 1995; Boudreau, 1996; Trinh *et al.*, 2000). Although there are some fluctuations in the data, Fig. 6 is consistent with the literature.

The data of Fig. 6 were converted into a logarithmic F-ϕ plot (Archie plot) using Eq. (4). Fig. 7 shows that the formation factor increases with decreasing porosity. This is a consequence of the obstruction effect of sand grains with $\rho = \infty$ on the electrical conductivity of the porous media system. The regression line, F =

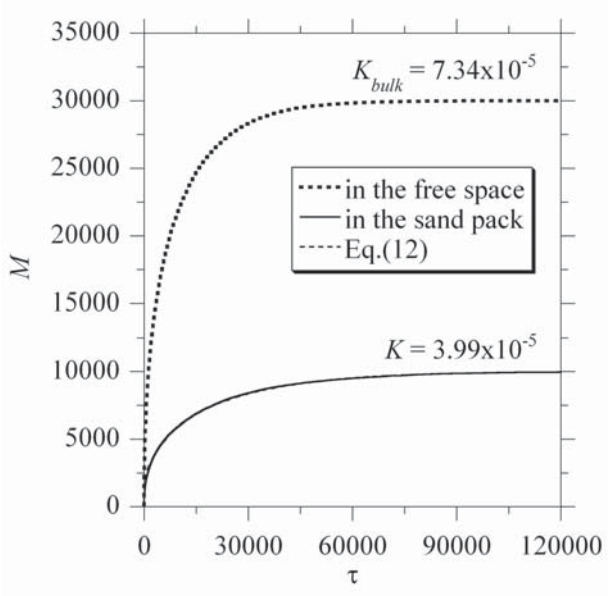

Fig. 5 Results for the lattice walk simulation through the pore space of the bead pack. Cumulated flux $M(\tau)$ for NumberOfDivision = 1, NumberOfWalkers = 30000, PixelRange = -1 to 58.5, and MaxTime = 200000. Data points for $\tau \leq 3000$ were discarded in fitting the data to Eq. (12) to reduce the error caused by truncation. It is difficult to distinguish the data points and Eq. (12) owing to the accuracy of the fit. Estimated K is indicated. Data from Fig. 4b are superimposed for reference.

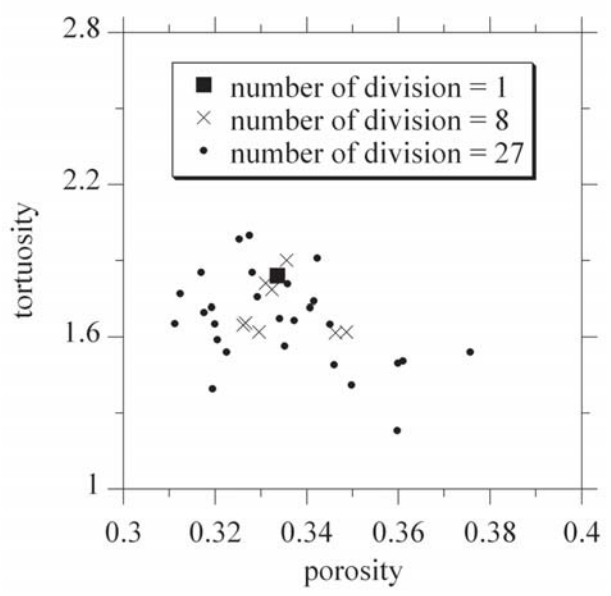

Fig. 6 Distribution of porosity and tortuosity in each sub-cube. The total number of sub-cubes determined by NumberOfDivision is indicated. The input values for NumberOfWalkers and PixelRange are identical to those for Fig. 5.

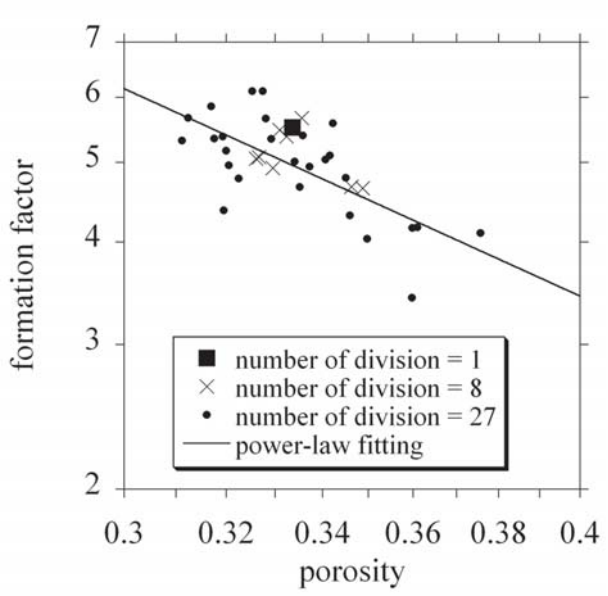

Fig. 7 Archie plot of Fig. 6. The formation factor was calculated by Eq. (4). The least-squares fitting was applied to the data points for "number of division = 27" to obtain $F = 0.54\ \phi^{-2.0}$ and indicated by a solid line.

$0.54\ \phi^{-2.0}$, is similar to those obtained by laboratory experiments (Jinguuji and Kunimatsu, 1999), demonstrating that DMAP.m is also useful for the estimate of the formation factors of porous media.

Our random walk program was therefore applied successfully to the 3D mapping of tortuosity, porosity, and formation factor in a bead pack. One of the advantages of diffusion simulation over conventional laboratory experiments (*e.g.*, Shackelford, 1991) is the significant saving in time by eliminating time-consuming practical steps (*e.g.*, slicing the sample into thin sections, extracting target species, and determining the concentration). It should be noted that the simulation time (about one day for Figs. 4-6) is much shorter than the time required for conventional laboratory diffusion experiments (typically several weeks). The digital image acquisition time for X-ray CT or MRI is also as short as several hours. Thus, computer simulation using digital images can be expected to reduce the acquisition time for diffusion data. It is hoped that making this program freely available will also facilitate diffusion studies on rock and sediment samples in many fields of geoscience.

Acknowledgement- Comments by an anonymous reviewer were helpful. Gratitude is extended to Dr. T. Nakano for helpful comments on Eqs. (5)-(8). The granodioritic sand samples were collected with the help by Dr. M. Yamamoto (Kagoshima University). This study was supported financially by the Ministry of Economy, Trade and Industry of Japan.

References

Boudreau, B.P. (1996) The diffusive tortuosity of fine-grained unlithified sediments. *Geochim. Cosmochim. Acta*, **60**, 3139-3142.

Crank, J. (1975) *The Mathematics of Diffusion*. Oxford University Press, Oxford, 414p.

Gibbs, S.J., Attard, J.J. and Hall, L.D. (1993) Diffusion in brine-saturated reservoir cores studied by NMR imaging. *AIChE J.*, **39**, 689-694.

Gleeson, J.W. and Woessner, D.E. (1991) Three-dimensional and flow-weighted NMR imaging of pore connectivity in a limestone. *Magn. Reson. Imaging*, **9**, 879-884.

Guéguen, Y. and Palciauskas, V. (1994) *Introduction to the Physics of Rocks*, Princeton University Press, Princeton, 392 p.

Hespe, E.D. (1971) Leach testing of immobilized radioactive waste solids. *Atom. Energy Rev.*, **9**, 195-207.

Jinguuji, M. and Kunimatsu, S. (1999) The measurement of liquefaction phenomena by resistivity and its evaluation. *BUTSURI-TANSA*, **52**, 439-445. (in Japanese with English abstract)

Jinguuji, M., Kunimatsu, S., Imaizumi, H., Tujino, S., and Maeda, S. (2003) Resistivity monitoring of liquefaction state during the in-situ blast testing. *BUTSURI-TANSA*, **56**, 149-155. (in Japanese with English abstract)

Latour, L.L., Mitra, P.P., Kleinberg, R.L. and Sotak, C.H. (1993) Time-dependent diffusion coefficient of fluids in porous media as a probe of surface-to-volume ratio. *J. Magn. Reson.*, **A101**, 342-346.

Nakashima, S. (1995) Diffusivity of ions in pore water as a quantitative basis for rock deformation rate estimates. *Tectonophys.*, **245**, 185-203.

Nakashima, Y. (2003a) Diffusion of H_2O in smectite gels: Obstruction effects of bound H_2O layers. *Clays Clay Min.*, **51**, 9-22.

Nakashima, Y. (2003b) Errata. *Clays Clay Min.*, **51**, 357.

Nakashima, Y. and Watanabe, Y. (2002) Estimate of transport properties of porous media by micro-focus X-ray computed tomography and random walk simulation. *Water Resour. Res.*, **38**, article number 1272, DOI number 10.1029/2001WR000937.

Nakashima, Y. and Yamaguchi, T. (2004) Original free Mathematica® programs for the calculation of transport properties of porous media. *In* Otani, J. and Obara, Y., eds., *X-ray CT for Geomaterials; Soils*, *Concrete*, *Rocks*. (A. A. Balkema Publishers), 103-110.

Nakashima, Y., Nakano, T., Nakamura, K., Uesugi, K., Tsuchiyama, A., and Ikeda, S. (2004) Three-dimensional diffusion of non-sorbing species in porous sandstone: Computer simulation based on X-ray microtomography using synchrotron radiation. *J. Contam. Hydrol.*, **74**, 253-264.

Sardini, P., Delay, F., Hellmuth, K.-H., Porel, G. and Oila, E. (2003) Interpretation of out-diffusion experiments on crystalline rocks using random walk modeling. *J. Contam. Hydrol.*, **61**, 339-350.

Shackelford, C.D. (1991) Laboratory diffusion testing for waste disposal-A review. *J. Contam. Hydrol.*, **7**, 177-217.

Siitari-Kauppi, M., Lindberg, A., Hellmuth, K.H., Timonen, J., Väätäinen, K., Hartikainen, J. and Hartikainen, K. (1997) The effect of microscale pore structure on matrix diffusion-a site-specific study on tonalite. *J. Contam. Hydrol.* **26**, 147-158.

Stauffer, D. (1985) *Introduction to Percolation Theory*. Taylor&Francis, London, 124p.

Trinh, S., Arce, P. and Locke, B. (2000) Effective diffusivities of point-like molecules in isotropic porous media by Monte Carlo simulation. *Transp. Porous Media.*, **38**, 241-259.

Watanabe, Y. and Nakashima, Y. (2002) RW3D.m: Three-dimensional random walk program for the calculation of the diffusivities in porous media. *Comput. Geosci.*, **28**, 583-586.

Watanabe, Y., Nakashima, Y. and Ohtani, T. (1999) 3D-Image processing program for the calculation of the volume histogram of cavities in rock samples. *J. Geotherm. Res. Soc. Japan*, **21**, 181-188.

Wildenschild, D., Hopmans, J.W., Vaz, C.M.P., Rivers, M.L., Rikard, D. and Christensen, B.S.B. (2002) Using X-ray computed tomography in hydrology: systems, resolutions, and limitations. *J. Hydrol.*, **267**, 285-297.

Received May 11, 2004
Accepted June 24, 2004

DMAP.m: 多孔質媒体中の屈曲度と空隙率の3次元分布を調べるためのMathematica®プログラム

中島善人・山口　哲

要　旨

等方的で不均一な多孔質媒体の空隙構造パラメータ（屈曲度と空隙率）を3次元マッピングする機能をもつ Mathematica プログラムを作成した．そのプログラム，DMAP.m は，パッケージタイプのプログラムで，Mathematica バージョン4あるいはそれ以降で動作する．DMAP.m は，X線CTや核磁気共鳴イメージングで取得した，多孔質堆積物や岩石等の3次元画像を読み込む．読み込んだ画像はサブシステムに細分化され，各サブシステムの空隙にランダムに散布された非吸着性のランダムウォーカーが酔歩（単純立方格子上の lattice walk）で系外に漏れ出ていくという，いわゆる out-diffusion シミュレーションを行う．系外に漏れたウォーカーの積算値の時間変動データをもちいて屈曲度を計算し，酔歩の出発点をランダムに選ぶ過程で空隙の画素にヒットした確率として空隙率を計算した（モンテカルロ積分）．このプログラムのデモンストレーションとして，ランダムパッキングした砂質堆積物のCT画像を用いて，屈曲度と空隙率のサブシステムサイズ依存性を計算した．なお，このプログラムは，http://staff.aist.go.jp/nakashima.yoshito/progeng.htmで無料ダウンロードできる．